A Heterogeneous Cellular Network Model with Inter-tier Dependence

Na Deng, Wuyang Zhou
Dept. of Electronic Engineering and Information Science
University of Science and Technology of China
Hefei, Anhui, 230026, China
Email:ndeng@mail.ustc.edu.cn, wyzhou@ustc.edu.cn

Martin Haenggi
Dept. of Electrical Engineering
University of Notre Dame
Notre Dame, IN, 46556, USA
Email:mhaenggi@nd.edu

***Abstract*—In heterogeneous cellular networks (HCNs), the macrocell network is usually assumed to be overlaid by multiple independent tiers of small cells. However, in reality, the locations of the base stations (BSs) belonging to different tiers are not fully independent. Accordingly, in this paper, we propose a two-tier HCN model with inter-tier dependence, where the macro-BS (MBS) and the pico-BS (PBS) deployments follow a Poisson point process (PPP) and a Poisson hole process (PHP), respectively. Under this setup, we derive bounds on the outage probabilities of both macro users and pico users, and then use a fitted Poisson cluster process to approximate the PHP, which is shown to provide a good approximation of the interference and outage. The results show that the model with inter-tier dependence appears closer to the real deployment than the two extremes with full regularity (the triangular lattice) and complete randomness (the PPP). An important conclusion is that significant gains can be obtained if PBSs are deployed smartly (away from MBSs).**

I. Introduction

To meet the crushing demands for mobile data traffic and universal seamless coverage, cellular networks are currently undergoing a major transformation from a thoroughly planned deployment to more irregular, heterogeneous deployments of macro-, pico- and femto-base stations (BSs) [1]. This increasing heterogeneity and density in cellular networks renders the traditional hexagonal and regular deployment models of limited utility but, in turn, motivates recent studies, tools and results inspired by stochastic geometry [2–4]. Most of the stochastic geometry work on cellular networks, due to its tractability, focus on the case where the BS deployment follows a homogeneous Poisson point process (PPP) for single-tier networks [5], or multiple tiers of mutually independent PPPs for heterogeneous cellular networks (HCNs) [6]. This means different types of BSs (e.g., macro BSs (MBSs) and pico BSs (PBSs)) are located independently of each other, which does not seem realistic since the locations of the BSs belonging to different tiers can be expected to exhibit some degree of repulsion. Therefore, models for HCNs accounting the inter-tier dependence should be devised and analyzed. This is the motivation of our work.

Significant efforts have been made recently on the modeling of HCNs by both academia and industry. An increasingly popular approach is to use random spatial models from stochastic geometry to capture the irregular network topology of HCNs. The model with K independent tiers of PPP distributed BSs is by far the most well-understood general HCN model in the literature due to its simplicity and tractability [6–8]. However, although there is randomness in the locations of small cells due to the variable capacity demand across the coverage area, it is unrealistic to assume that the positions of the BSs belonging to different tiers are completely uncorrelated. This is because the BSs are deployed through a sophisticated network planning procedure, which results in correlations between the multiple tiers. To our best knowledge, almost no works have so far allowed a multi-tier HCN model with inter-tier dependence from stochastic geometry except the classical grid models in which the locations of the BSs can be thoroughly planned (see, e.g., [9], where the PBSs are regularly deployed at the cell edge of each MBS). Nevertheless, due to the inherent complexity and randomness of HCNs, the network performance of the grid model is typically evaluated by system-level simulations, since no analytical approaches are available.

In this paper, considering the accuracy, tractability and practicability tradeoffs, we propose a two-tier HCN model with inter-tier dependence with two types of BSs, i.e., MBSs and PBSs, using two correlated spatial point processes, where a PBS is deployed only when it is outside the MBS exclusion regions. This model, to some extent, also helps reduce the inter-tier interference (because of the exclusion region), which is one of the major challenges of HCNs. Under this setup, the MBS and the PBS deployments follow a PPP and a Poisson hole process (PHP) [2, Section 3.3], respectively. Due to the inter-tier dependence, an exact calculation of the interference and outage probability seems unfeasible. Instead, two different approaches are taken to tackle this problem: one is to derive bounds on the outage probabilities of both macro users (MUs) and pico users (PUs), and the other is to approximate the PHP using fitted Poisson cluster processes (PCPs). Both approaches have their own strengths and weaknesses. The bounds are tight and have closed-form expressions that are easy to calculate. On the other hand, the approximations using fitted point processes can provide us with a complete topology of the network deployments even though the resulting expressions involve multiple integrals.

From a broader perspective, the contribution of the paper lies in the investigation of a novel model with inter-tier dependence for HCNs, which is applicable to actual network

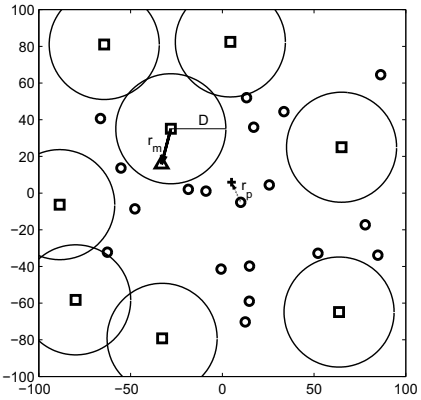

Fig. 1. The two-tier HCN model. The squares are the MBSs and the triangle is the typical macro user at a distance r_{m} from its serving MBS in a random direction. The big circles are the exclusion regions with radius D. The small circles are the PBSs deployed outside the exclusion regions and the '+' is the typical pico user at a distance r_{p} from its serving PBS in a random direction.

deployments, and the bounds and approximations obtained provide useful insights into the analysis and design of future wireless networks.

II. Network Model

Consider a two-tier HCN with two types of BSs, i.e., MBSs overlaid with PBSs, shown in Figure 1. The locations of the MBSs follow a homogeneous PPP $\Phi_{\mathrm{m}} = \{x_1, x_2, \ldots\} \subset \mathbb{R}^2$ of density λ_{m}, and the *potential* locations of the PBSs follow another independent homogeneous PPP $\widetilde{\Phi}_{\mathrm{p}} = \{y_1, y_2, \ldots\} \subset \mathbb{R}^2$ of density $\widetilde{\lambda}_{\mathrm{p}}$. Each MBS has an exclusion region which is a circular region with radius D centered at the location of the MBS. Considering the critical issues of the current HCNs, such as interference, resource utilization and economy, only the PBSs whose locations are outside the exclusion regions are deployed to improve the network capacity, fill the coverage holes, and thus provide better service to users, while guaranteeing that PBSs will, on average, not generate an aggregate interference resulting in the outage of macro users through designing the exclusion radius D. Under this setup, the PBSs form a point process called the *Poisson hole process*, which is a Cox process and has been used for cognitive networks [10]. We denote this process by $\Phi_p \subset \widetilde{\Phi}_p$ and define it as follows.

Definition 1. ***(Poisson hole process, PHP** [2, Example 3.7]) Let Φ_1 be a* PPP *of intensity λ_1 and Φ_2 be a* PPP *of intensity λ_2, $\lambda_2 > \lambda_1$. For each $x \in \Phi_1$, remove all the points in $\Phi_2 \bigcap b(x, D)$, where $b(x, D)$ is a ball centered at x with radius D. Then, the remaining points of Φ_2 form the Poisson hole process. Its intensity is $\lambda = \lambda_2 \exp(-\lambda_1 \pi D^2)$.*

The transmission power is μ_{m} for each MBS and μ_{p} for each PBS. The power received by a receiver located at z due to a transmitter at x is modeled as $h_x \ell(x - z)$, where h_x is the power fading coefficient (square of the amplitude fading coefficient) associated with the channel between x and z. We assume that the fading coefficients are i.i.d. exponential (Rayleigh fading) with $\mathbb{E}[h] = 1$. $\ell(x) = \|x\|^{-\alpha}$ is the large-scale path loss model with $\alpha > 2$. We focus on a macro user at a distance $r_{\mathrm{m}} < D$ from the serving MBS in a random direction and on a pico user at a distance r_{p} from the serving PBS in a random direction. r_{p} is assumed to be small relative to the mean nearest-neighbor distance of $\widetilde{\Phi}_{\mathrm{p}}$ (i.e., $r_{\mathrm{p}} \ll \widetilde{\lambda}_{\mathrm{p}}^{-\frac{1}{2}}$) since the transmission power and the range of the PBSs are usually small. The signal-to-interference ratio (SIR) threshold is denoted as θ_{m} for macro users and θ_{p} for pico users.

The radius D of the exclusion region is chosen as

$$D = \zeta r_{\mathrm{m}} \left[\theta_{\mathrm{m}} \left(\frac{\mu_{\mathrm{p}}}{\mu_{\mathrm{m}}}\right)\right]^{\frac{1}{\alpha}}, \tag{1}$$

where ζ is a design factor. This form of D is chosen since the radius D should be positively related to the distance r_{m} between the serving MBS and its user, the SIR threshold θ_{m}, and the transmission power of the PBSs μ_{p}, and inversely related to the transmission power of the MBSs μ_{m}. The path loss exponent should also be taken into account since it greatly affects the interference. Adding a design parameter ζ makes the formula of D more general; it also resembles the concept of *Cell Range Expansion* (CRE), i.e., allowing a user to be served by a cell with weaker received power [11]. For our model, we can control the offloading from the macro to pico cells through adjusting the size of the exclusion region, which determines the number of PBSs that can be retained in the HCNs. When D is set relatively large, very few potential PBSs will be retained and most users are served by the MBSs. Conversely, when D is small, the retaining PBSs will offload more traffic from the macro cell. Note that D is designed to guarantee that PBSs will, on average, not generate an aggregate interference resulting in the outage of macro users, which occurs when the instantaneous SIR is lower than θ_{m}. Similarly, the MBSs will, on average, not generate an aggregate interference resulting in the outage of PUs since the minimum distance between a MBS and a PU is $D - r_{\mathrm{p}}$.

III. Analysis of the Two-tier HCN Model with Inter-tier Dependence

In this section, the two-tier HCN model with the inter-tier dependence is discussed. We first analyze the aggregate interference to both MUs and PUs, including the intra-tier interference and the inter-tier interference, and then give the bounds on the outage probabilities of MUs and PUs, respectively.

There are four types of interference: the interference from the MBSs to the MUs I_{mm}, the interference from the MBSs to the PUs I_{mp}, the interference from the PBSs to the MUs I_{pm}, and the interference from the PBSs to the PUs I_{pp}. Each of them can be defined as $I(z) = \sum_{x \in \Phi \setminus \{x_0\}} \mu h_x \ell(z - x)$ to represent the interference at z resulting from the interferers positioned at the points of the process Φ (i.e., either Φ_{m} or Φ_{p}), where x_0 is the serving BS, and μ is either μ_{m} or

$\mu_{\rm p}$, depending on which type of interference is considered. To calculate the interference to the MUs, we condition on having a MU at the origin, the *typical user*, i.e., there is an extra MBS, namely, the serving MBS, on the circle of radius $r_{\rm m}$ centered at o, which yields the Palm distribution for the MBSs. By Slivnyak's theorem [2], this conditional distribution is the same as the original one for the macro-tier in the region $\mathbb{R}^2 \setminus b(o, r_{\rm m})$. For the pico-tier, however, conditioning on a PBS at a certain location generally changes the distance distribution since whether a PBS is deployed is determined by the locations of the MBSs. This is the reason why only bounds or approximations through fitting the Poisson cluster process (PCP) can be obtained for the interference terms involving the PBSs.

A. Interference and Outage Analysis of MUs

The MUs suffer from two types of interference: $I_{\rm mm}$ and $I_{\rm pm}$. The typical MU is assumed to access the nearest MBS x_0 at distance $r_{\rm m}$. Since the fading is Rayleigh and the MBSs are distributed as a PPP, the Laplace transform of $I_{\rm mm}$ is

$$\begin{aligned}\mathcal{L}_{I_{\rm mm}}(s) &= \mathbb{E}^{!x_0}_{\Phi_{\rm m},h_x}\left(\exp\left(-s\sum_{x\in\Phi_{\rm m}}\mu_{\rm m}h_x\ell(x)\right)\right)\\ &= \exp\left(-\pi\lambda_{\rm m}\int_{r_{\rm m}^2}^{\infty}\frac{1}{1+s^{-1}\mu_{\rm m}^{-1}r^{\alpha/2}}{\rm d}r\right). \quad (2)\end{aligned}$$

Since the PBSs must be at least at distance D from the MBSs, $I_{\rm pm}$ is stochastically dominated[1] by the interference $\hat{I}_{\rm pm}$ caused by the points in $\widetilde{\Phi}_{\rm p}$ except those that are within the distance D from the desired MBS. Denote the disk centered at the location of the desired MBS with radius D as $\mathcal{H}_{\rm m}$ and let $\mathcal{H}_{\rm m}^{\mathcal{C}} = \mathbb{R}^2 \setminus \mathcal{H}_{\rm m}$. We obtain the Laplace transform of the $\hat{I}_{\rm pm}$ using a modified path loss law $\widetilde{\ell}(x) = \ell(x)\mathbf{1}_{x\in\mathcal{H}_{\rm m}^{\mathcal{C}}}$ as

$$\begin{aligned}\mathcal{L}_{\hat{I}_{\rm pm}}(s) &= \mathbb{E}_{\Phi_{\rm m},h_x}\left(\exp\left(-s\sum_{x\in\widetilde{\Phi}_{\rm p}}\mu_{\rm p}h_x\widetilde{\ell}(x)\right)\right)\\ &= \exp\left(-\widetilde{\lambda}_{\rm p}\int_{\mathbb{R}^2}1-\frac{1}{1+s\mu_{\rm p}\widetilde{\ell}(x)}{\rm d}x\right)\\ &= \exp\left(-\widetilde{\lambda}_{\rm p}\int_{\mathcal{H}_{\rm m}^{\mathcal{C}}}\frac{s\mu_{\rm p}\ell(x)}{1+s\mu_{\rm p}\ell(x)}{\rm d}x\right)\\ &= \exp\left\{-\widetilde{\lambda}_{\rm p}\left(\frac{\pi^2\delta}{\sin(\pi\delta)}\mu_{\rm p}^{\delta}s^{\delta}-\pi D^2(1-A_{\rm m}(s,D))\right)\right\},\end{aligned} \quad (3)$$

where $\delta = 2/\alpha$ and

$$\begin{aligned}A_{\rm m}(s,D) &= \frac{1}{\pi D^2}\int_{\mathcal{H}_{\rm m}}\frac{1}{1+s\mu_{\rm p}\ell(|x|)}{\rm d}x\\ &= \frac{1}{\pi D^2}\int_0^{2\pi}\int_0^{r_{\rm m}\cos\varphi+\sqrt{D^2-r_{\rm m}^2\sin^2\varphi}}\frac{r}{1+s\mu_{\rm p}r^{-\alpha}}{\rm d}r{\rm d}\varphi.\end{aligned} \quad (4)$$

[1]A random variable A stochastically dominates a random variable B if $\mathbb{P}(A > x) \geq \mathbb{P}(B > x)$ for all x, or equivalently, $F_A(x) \leq F_B(x)$ for cumulative distribution functions $F_A(x)$ and $F_B(x)$.

With Rayleigh fading, the transmission success probability of the MU is the Laplace transform evaluated at $s = \theta_{\rm m}\mu_{\rm m}^{-1}r_{\rm m}^{\alpha}$. Since the MBSs and the potential PBSs are distributed according to two independent PPPs, $I_{\rm mm}$ and $\widehat{I}_{\rm pm}$ are independent. Therefore, an upper bound for the outage probability of MUs, denoted as $\epsilon_{\rm m}$, is given by

$$\epsilon_{\rm m} < 1 - \mathcal{L}_{I_{\rm mm}}(\theta_{\rm m}\mu_{\rm m}^{-1}r_{\rm m}^{\alpha})\mathcal{L}_{\hat{I}_{\rm pm}}(\theta_{\rm m}\mu_{\rm m}^{-1}r_{\rm m}^{\alpha}). \quad (5)$$

When $\alpha = 4$, the above bound can be simplified to

$$\begin{aligned}\epsilon_{\rm m} < 1-\exp\Bigg\{-\pi\sqrt{\theta_{\rm m}}r_{\rm m}^2\Big(\lambda_{\rm m}\arctan\sqrt{\theta_{\rm m}}+\\ \widetilde{\lambda}_{\rm p}\Big(\frac{\pi}{2}\sqrt{\frac{\mu_{\rm p}}{\mu_{\rm m}}}-\frac{D^2}{\sqrt{\theta_{\rm m}}r_{\rm m}^2}\big(1-A_{\rm m}(\theta_{\rm m}\mu_{\rm m}^{-1}r_{\rm m}^4,D)\big)\Big)\Big)\Bigg\}.\end{aligned} \quad (6)$$

Although the point process of the PBSs is not a PPP but a Poisson hole process (see Def. 1 in Section II), independent thinning of $\widetilde{\Phi}_{\rm p}$ outside the exclusion regions with probability $\exp(-\lambda_{\rm m}\pi D^2)$ yields a good approximation on $I_{\rm pm}$, since the higher-order statistics of the point processes, which govern the interaction between nodes, become less relevant further away from the receiver [12]. An approximation to the outage probability of MUs $\epsilon_{\rm m}$ is, therefore, given by

$$\epsilon_{\rm m} \approx 1 - \mathcal{L}_{I_{\rm mm}}(\theta_{\rm m}\mu_{\rm m}^{-1}r_{\rm m}^{\alpha})\mathcal{L}_{\widetilde{I}_{\rm pm}}(\theta_{\rm m}\mu_{\rm m}^{-1}r_{\rm m}^{\alpha}), \quad (7)$$

where the Laplace transform of the approximation $\widetilde{I}_{\rm pm}$ is

$$\mathcal{L}_{\widetilde{I}_{\rm pm}}(s)=\exp\left\{-\lambda_{\rm p}\left(\frac{\pi^2\delta}{\sin(\pi\delta)}\mu_{\rm p}^{\delta}s^{\delta}-\pi D^2(1-A(s,D))\right)\right\}. \quad (8)$$

When $\alpha = 4$, the above approximation can be simplified to

$$\begin{aligned}\epsilon_{\rm m}\approx1-\exp\Bigg\{-\pi\sqrt{\theta_{\rm m}}r_{\rm m}^2\Big(\lambda_{\rm m}\arctan\sqrt{\theta_{\rm m}}+\\ \lambda_{\rm p}\Big(\frac{\pi}{2}\sqrt{\frac{\mu_{\rm p}}{\mu_{\rm m}}}-\frac{D^2}{\sqrt{\theta_{\rm m}}r_{\rm m}^2}\big(1-A_{\rm m}(\theta_{\rm m}\mu_{\rm m}^{-1}r_{\rm m}^4,D)\big)\Big)\Big)\Bigg\}.\end{aligned} \quad (9)$$

B. Interference and Outage Analysis of PUs

Similar to the case of the estimating interference to the MUs, the PU also experiences two types of interference: $I_{\rm mp}$ and $I_{\rm pp}$. First, we consider the interference $I_{\rm mp}$. The typical PU is assumed to access the nearest PBS at distance $r_{\rm p}$. Denote $\mathcal{H}_{\rm p}$ as the disk centered at the location of the desired PBS with radius D and $\mathcal{H}_{\rm p}^{\mathcal{C}} = \mathbb{R}^2 \setminus \mathcal{H}_{\rm p}$, thus we have

$$\mathcal{L}_{I_{\rm mp}}(s)=\exp\left\{-\lambda_{\rm m}\left(\frac{\pi^2\delta}{\sin(\pi\delta)}\mu_{\rm m}^{\delta}s^{\delta}-\pi D^2(1-A_{\rm p}(s,D))\right)\right\}, \quad (10)$$

where

$$A_{\rm p}(s,D)=\frac{1}{\pi D^2}\int_0^{2\pi}\int_0^{r_{\rm p}\cos\varphi+\sqrt{D^2-r_{\rm p}^2\sin^2\varphi}}\frac{r}{1+s\mu_{\rm m}r^{-\alpha}}{\rm d}r{\rm d}\varphi. \quad (11)$$

Now let us consider the interference from other PBSs $I_{\rm pp}$. Let $\hat{I}_{\rm pp}$ be the interference caused by the points in $\widetilde{\Phi}_{\rm p}$ except those that are within the distance $r_{\rm p}$ from the typical PU, thus $I_{\rm pp}$ is stochastically dominated by $\hat{I}_{\rm pp}$, and its Laplace transform is $\mathcal{L}_{\hat{I}_{\rm pp}}(s) = \exp\left(-\pi\widetilde{\lambda}_{\rm p}\int_{r_{\rm p}^2}^{\infty}\frac{1}{1+s^{-1}\mu_{\rm p}^{-1}r^{\alpha/2}}{\rm d}r\right)$.

The success transmission probability of PUs is the Laplace transform evaluated at $s = \theta_{\rm p}\mu_{\rm p}^{-1}r_{\rm p}^{\alpha}$. Since $I_{\rm mp}$ and $\widehat{I}_{\rm pp}$ are independent, an upper bound for the outage probability of PUs, denoted as $\epsilon_{\rm p}$, can be obtained as

$$\epsilon_{\rm p} < 1 - \mathcal{L}_{I_{\rm mp}}(\theta_{\rm p}\mu_{\rm p}^{-1}r_{\rm p}^{\alpha})\mathcal{L}_{\hat{I}_{\rm pp}}(\theta_{\rm p}\mu_{\rm p}^{-1}r_{\rm p}^{\alpha}). \tag{12}$$

When $\alpha = 4$, the above bound can be simplified to

$$\epsilon_{\rm p}<1-\exp\Bigg\{-\pi\sqrt{\theta_{\rm p}}r_{\rm p}^2\Bigg(\lambda_{\rm p}\arctan\sqrt{\theta_{\rm p}}+ \lambda_{\rm m}\left(\frac{\pi}{2}\sqrt{\frac{\mu_{\rm m}}{\mu_{\rm p}}}-\frac{D^2}{\sqrt{\theta_{\rm p}}r_{\rm p}^2}\left(1-A_{\rm p}(\theta_{\rm p}\mu_{\rm p}^{-1}r_{\rm p}^4,D)\right)\right)\Bigg)\Bigg\}. \tag{13}$$

C. Comparison with the Two-tier Independent PPP Model

When the PBSs are distributed independently of the MBSs, the outage probability for both types of users can be easily obtained as

$$\epsilon_{\rm m} = 1 - \exp\left\{-\pi\lambda_{\rm m}\int_{r_{\rm m}^2}^{\infty}\frac{1}{1+\theta_{\rm m}^{-1}r_{\rm m}^{-\alpha}r^{\alpha/2}}{\rm d}r - \frac{\pi^2\delta}{\sin(\pi\delta)}\theta_{\rm m}^{\delta}r_{\rm m}^2\lambda_{\rm p}(\mu_{\rm p}/\mu_{\rm m})^{\delta}\right\}, \tag{14}$$

$$\epsilon_{\rm p} = 1 - \exp\left\{-\frac{\pi^2\delta}{\sin(\pi\delta)}\theta_{\rm p}^{\delta}r_{\rm p}^2\lambda_{\rm m}(\mu_{\rm m}/\mu_{\rm p})^{\delta} -\pi\lambda_{\rm p}\int_{r_{\rm p}^2}^{\infty}\frac{1}{1+\theta_{\rm p}^{-1}r_{\rm p}^{-\alpha}r^{\alpha/2}}{\rm d}r\right\}. \tag{15}$$

When $\alpha = 4$, the above results can be simplified to

$$\epsilon_{\rm m}=1-\exp\left\{-\pi\sqrt{\theta_{\rm m}}r_{\rm m}^2\left(\lambda_{\rm m}\arctan\sqrt{\theta_{\rm m}}+\frac{\pi}{2}\lambda_{\rm p}\sqrt{\frac{\mu_{\rm p}}{\mu_{\rm m}}}\right)\right\} \tag{16}$$

$$\epsilon_{\rm p}=1-\exp\left\{-\pi\sqrt{\theta_{\rm p}}r_{\rm p}^2\left(\frac{\pi}{2}\lambda_{\rm m}\sqrt{\frac{\mu_{\rm m}}{\mu_{\rm p}}}+\lambda_{\rm p}\arctan\sqrt{\theta_{\rm p}}\right)\right\} \tag{17}$$

IV. Approximation by Poisson Cluster Process

The PHP behaves like a PCP to some extent, since forming "holes", due to the exclusion regions in our model, forces nodes to concentrate in other parts, making the whole node distribution look as if the nodes were clustered. Based on this, in this section, we provide another approach to approximate the outage performance of both types of users: since the PHP is not very tractable, we approximate it with a PCP by matching first- and second-order statistics. Figure 2 illustrates a PHP and a TCP with the same first- and second-order statistics. It is easy to observe that both processes are very different from the PPP.

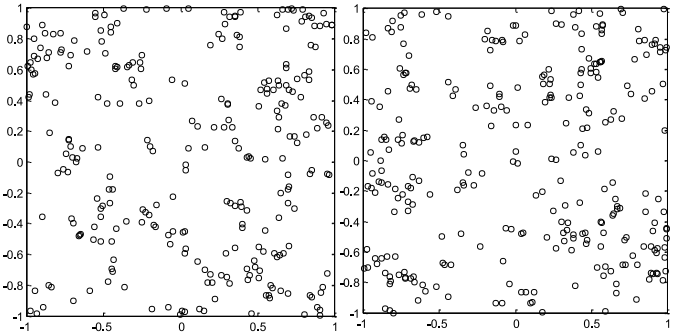

Fig. 2. Comparison of the PHP (left) and TCP (right). For the PHP, $\lambda_{\rm m} = 25$, $\widetilde{\lambda}_{\rm p} = 150$, $\mu_{\rm m} = 1$, $\mu_{\rm p} = 0.05$, $r_{\rm m} = 0.04$, $r_{\rm p} = 0.01$, $\zeta = 3$, $\alpha = 4$, $\theta_{\rm m} = 10{\rm dB}$, $D = 0.101$. For the TCP, $\lambda_l = 35.4382$, $\bar{c} = 1.9024$, $\sigma^2 = 0.0023$.

A. Fitting a Poisson Cluster Process

The first-order statistic is the intensity, so

$$\lambda_{\rm p} = \widetilde{\lambda}_{\rm p}\exp(-\lambda_{\rm m}\pi D^2) = \lambda_l\bar{c}, \tag{18}$$

where $\lambda_{\rm p}$ is the intensity of the PBSs; λ_l is the density of parent points of the cluster process, and $\bar{c}$ is the average number of points in a cluster. For motion-invariant processes, the second-order statistics are fully described by the pair-correlation function $g(r)$ [2]. Here two kinds of Poisson cluster processes are considered: the Matern cluster process (MCP) and the Thomas cluster process (TCP).

For a cluster radius R, the g-function of the MCP is [2, Section 6.4]

$$g_{\rm M}(r)=\begin{cases}1+\frac{2}{\lambda_l\pi^2R^2}\left[\arccos\left(\frac{r}{2R}\right)-\frac{r\sqrt{4R^2-r^2}}{4R^2}\right], & r<2R\\ 1, & r\geq 2R\end{cases} \tag{19}$$

where λ_l and R can be determined using curve-fitting to the g-function of the PHP. $\bar{c}$ is then determined using (18).

For the TCP with variance σ^2, the g-function is [2, Section 6.4]

$$g_{\rm T}(r) = 1 + \frac{1}{4\pi\lambda_l\sigma^2}\exp\left(-\frac{r^2}{4\sigma^2}\right), \tag{20}$$

where λ_l and σ are obtained using curve-fitting and $\bar{c}$ is then determined using (18).

To illustrate the fitting, we set $\lambda_{\rm m} = 1.59\times10^{-5}$, $\widetilde{\lambda}_{\rm p} = 1.59\times10^{-4}$, $r_{\rm m} = 40$, $r_{\rm p} = 10$, $\mu_{\rm m} = 1$, $\mu_{\rm p} = 0.05$, $\zeta = 3$, $\alpha = 4$. By using the **nlinfit** function (nonlinear least-squares fit) in Matlab, we fit the g-function of the TCP and MCP to that of the PHP for different $\theta_{\rm m}$, and the fitting results are listed in Table I. It can be seen that R increases as D increases, which means the clustering behavior is increasingly prominent as the exclusion region becomes larger. Figure 3 shows the g-function of the PHP, TCP, and MCP obtained by simulations for $\theta_{\rm m}=10, 15{\rm dB}$. The results show that the PHP can be closely approximated by the TCP and MCP.

TABLE I. The fitting results for different θ_{m}

	θ_{m}(dB)	-5	0	5	10	15	20
	D	42.55	56.74	75.67	100.91	134.56	179.44
Matern	λ_{l}	1.80×10^{-3}	5.81×10^{-4}	1.84×10^{-4}	5.65×10^{-5}	1.65×10^{-5}	4.54×10^{-6}
	R	43.76	58.13	72.55	95.25	120.91	144.72
	$\bar{c}$	0.080	0.247	0.672	1.749	3.995	7.131
Thomas	λ_{l}	1.70×10^{-3}	5.49×10^{-4}	1.78×10^{-4}	5.47×10^{-5}	1.61×10^{-5}	4.46×10^{-6}
	σ^2	585.15	1022.8	1542.6	2649.3	4225.0	5994.5
	$\bar{c}$	0.084	0.247	0.672	1.749	3.995	7.132

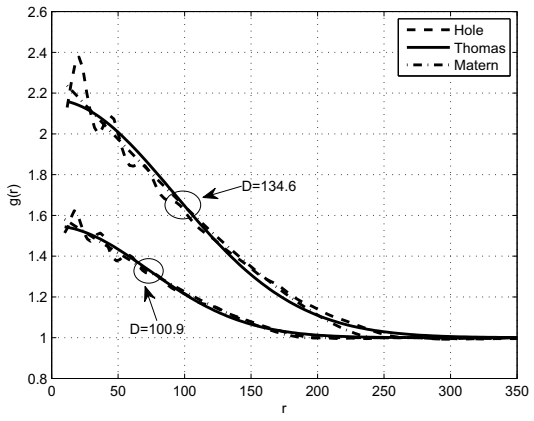

Fig. 3. Pair correlation function. $\lambda_{\mathrm{m}} = 1.59 \times 10^{-5}$, $\widetilde{\lambda}_{\mathrm{p}} = 1.59 \times 10^{-4}$, $r_{\mathrm{m}} = 40$, $r_{\mathrm{p}} = 10$, $\mu_{\mathrm{m}} = 1$, $\mu_{\mathrm{p}} = 0.05$, $\zeta = 3$, $\alpha = 4$.

B. Outage Analysis Using Poisson Cluster Process

Since the PHP can be closely approximated by a fitted PCP, the interference in the Poisson hole networks can be approximated by that in Poisson cluster networks.

Let $\mathcal{L}_{I_{\mathrm{pm,PCP}}}(s)$ be the Laplace transform of the interference from a PCP at the typical MU located at the origin. According to [13], we have

$$\mathcal{L}_{I_{\mathrm{pm,PCP}}}(s) = \exp\left\{-\lambda_l \int_{\mathbb{R}^2} [1 - \exp(-\bar{c}\nu(s,y))]\mathrm{d}y\right\}, \quad (21)$$

where

$$\nu(s,y) = \int_{\mathbb{R}^2} \frac{1}{1 + (s\mu_{\mathrm{p}}\widetilde{\ell}(x-y))^{-1}} f(x)\mathrm{d}x, \quad (22)$$

and $f(x)$ is the PDF of the node distribution around the parent point. For the TCP,

$$f(x) = \frac{1}{2\pi\sigma^2} \exp\left\{-\frac{\|x\|^2}{2\sigma^2}\right\}, \quad (23)$$

and for the MCP,

$$f(x) = \begin{cases} \frac{1}{\pi R^2}, & \|x\| < R \\ 0, & \text{otherwise} \end{cases} \quad (24)$$

Thus the outage probability of MUs can be derived as

$$\epsilon_{\mathrm{m}} \approx 1 - \mathcal{L}_{I_{\mathrm{mm}}}(\theta_{\mathrm{m}}\mu_{\mathrm{m}}^{-1} r_{\mathrm{m}}^{\alpha}) \mathcal{L}_{I_{\mathrm{pm,PCP}}}(\theta_{\mathrm{m}}\mu_{\mathrm{m}}^{-1} r_{\mathrm{m}}^{\alpha}). \quad (25)$$

Let $\mathcal{L}_{I_{\mathrm{pp,PCP}}}(s)$ be the Laplace transform of the interference from a PCP at the typical PU located at the origin. Since the typical PU is served by the nearest PBS located at $(r_{\mathrm{p}}, 0)$, there is no PBS in the disk region centered at the origin with radius r_{p}. Thus, by denoting the modified path loss law $\widetilde{\ell}(x) = \ell(x)\mathbf{1}_{\|x\|>r_{\mathrm{p}}}$ and according to [13], we have

$$\mathcal{L}_{I_{\mathrm{pp,PCP}}}(s) = \exp\left\{-\lambda_{\mathrm{l}} \int_{\mathbb{R}^2} [1 - \exp(-\bar{c}\nu(s,y))]\mathrm{d}y\right\} \times \int_{\mathbb{R}^2} \exp(-\bar{c}\nu(s,y)) f(y)\mathrm{d}y, \quad (26)$$

where

$$\nu(s,y) = \int_{\mathbb{R}^2} \frac{1}{1 + (\widetilde{\ell}(x-y)s\mu_{\mathrm{p}})^{-1}} f(x)\mathrm{d}x. \quad (27)$$

Thus, the outage probability of PUs can be obtained as

$$\epsilon_{\mathrm{p}} \approx 1 - \mathcal{L}_{I_{\mathrm{mp}}}(\theta_{\mathrm{p}}\mu_{\mathrm{p}}^{-1} r_{\mathrm{p}}^{\alpha}) \mathcal{L}_{I_{\mathrm{pp,PCP}}}(\theta_{\mathrm{p}}\mu_{\mathrm{p}}^{-1} r_{\mathrm{p}}^{\alpha}). \quad (28)$$

V. Numerical Results

In this section, we give some numerical results of the outage probability for MU and PU, respectively, where $\lambda_{\mathrm{m}} = 1.59 \times 10^{-5}$, $\widetilde{\lambda}_{\mathrm{p}} = 1.59 \times 10^{-4}$, $\mu_{\mathrm{m}} = 1$, $\mu_{\mathrm{p}} = 0.05$, $r_{\mathrm{m}} = 40$, $r_{\mathrm{p}} = 10$, $\zeta = 3$, $\alpha = 4$. Both approaches provided in Section III, i.e., bounds and approximations using the PCP, are investigated as well as the corresponding simulation results. For comparison, we also provide two cases with the same densities of the MBSs and PBSs: one is to model the HCN with two independent PPPs, and the other is to model the MBSs as a triangular lattice and the PBSs as a lattice hole process[2].

Figure 4 and Figure 5 illustrate the outage probability of MUs and PUs, respectively. It can be seen that the bounds derived for the outage probability of both types of UEs are quite tight, and the approximations using the fitted MCP and TCP match the simulation results very well, which verifies that the PCP can model the PHP accurately, and a good estimate of the interference can be obtained. We can also observe that the outage performance of the proposed model with inter-tier dependence falls somewhere in between those of the two extremes, i.e., complete randomness (the two-tier independent PPPs) and full regularity (the triangular lattice). Since it is well recognized that the PPP assumption for the spatial locations of the BSs provides an upper bound on the outage probability of actual BS deployment while the idealized grid-based model provides a lower bound [6], we may conclude that the model with the inter-tier dependence

[2]The lattice hole process is formed by retaining all the points of a PPP that outside the exclusion regions of the MBSs whose locations follow a triangular lattice.

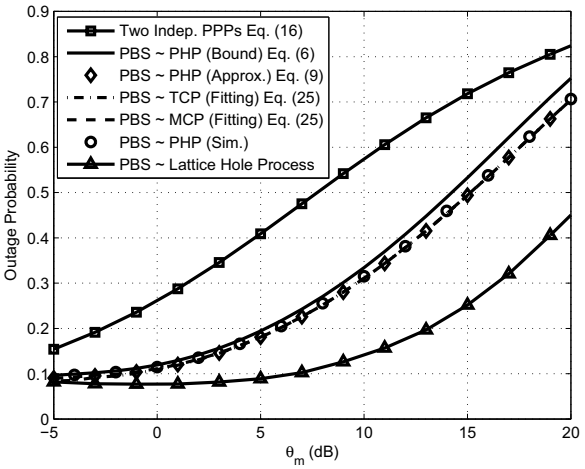

Fig. 4. The outage probability of MUs. The curve of the lattice hole process has a slight decrease for small θ_{m} since the interference from PBSs decreases with $D \propto \theta_{\mathrm{m}}^{1/\alpha}$, which more than offsets the increase in θ_{m} in this range.

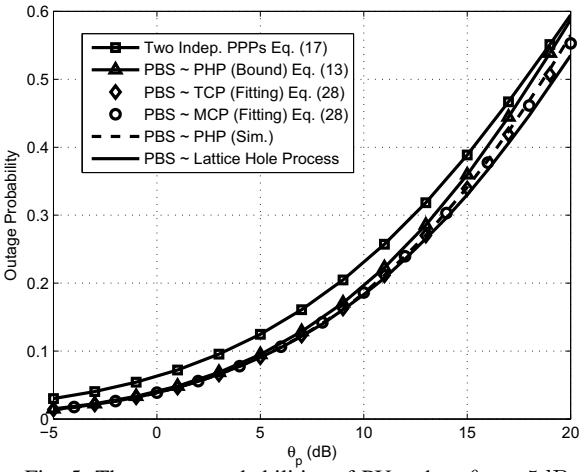

Fig. 5. The outage probabilities of PUs when $\theta_{\mathrm{m}} = 5\mathrm{dB}$.

appears closer to the real deployment than independent tiers of PPPs or grid-based models. In addition, comparing Figure 4 with Figure 5, we find that the performance of the MUs is affected by the inter-tier dependence more seriously than that of the PUs from the gap between the proposed model and the two extreme cases.

VI. Conclusion

In this paper, we propose a two-tier HCN model accounting for inter-tier dependence, where the MBSs and PBSs follow a PPP and a PHP, respectively. Due to the repulsion between the MBS tier and the PBS tier, the interference in the HCN is hard to analyze exactly. Thus, under this setup, we first bounded the outage probabilities of both MUs and PUs, and then used a fitted PCP to approximate the PHP. The results indicate that the bounds derived are very tight to the simulation curve and the approximations using the fitted PCPs coincide quite exactly with the simulation curve, thus providing useful approximations for a practical network model where an exact calculation of the interference is unfeasible. Besides, since the performance of the proposed model falls in between the performance of model with two-tier independent PPPs and that with triangular lattice consisting with the known results of actual deployment, we can conclude that the model with inter-tier dependence is a more promising HCN model than the two extremes with full regularity and complete and independent randomness. Overall, the bounds and approximations show that there is a significant gain in deploying PBSs smartly (away from MBSs).

Acknowledgment

The work of N. Deng and W. Zhou has been supported by National programs for High Technology Research and Development (2012AA011402), National Natural Science Foundation of China (61172088), and the work of M. Haenggi has been supported by the U.S. NSF (grants CNS 1016742 and CCF 1216407).

References

[1] A. Ghosh *et al.*, "Heterogeneous cellular networks: From theory to practice," *Communications Magazine, IEEE*, vol. 50, no. 6, pp. 54–64, 2012.

[2] M. Haenggi, *Stochastic geometry for wireless networks*. Cambridge University Press, 2012.

[3] H. ElSawy, E. Hossain, and M. Haenggi, "Stochastic geometry for modeling, analysis, and design of multi-tier and cognitive cellular wireless networks: A survey," *Communications Surveys & Tutorials, IEEE*, vol. 15, no. 3, pp. 996–1019, 2013.

[4] J. G. Andrews, R. K. Ganti, M. Haenggi, N. Jindal, and S. Weber, "A primer on spatial modeling and analysis in wireless networks," *Communications Magazine, IEEE*, vol. 48, no. 11, pp. 156–163, 2010.

[5] J. G. Andrews, F. Baccelli, and R. K. Ganti, "A tractable approach to coverage and rate in cellular networks," *Communications, IEEE Transactions on*, vol. 59, no. 11, pp. 3122–3134, 2011.

[6] H. S. Dhillon, R. K. Ganti, F. Baccelli, and J. G. Andrews, "Modeling and analysis of K-tier downlink heterogeneous cellular networks," *Selected Areas in Communications, IEEE Journal on*, vol. 30, no. 3, pp. 550–560, 2012.

[7] S. Mukherjee, "Distribution of downlink SINR in heterogeneous cellular networks," *Selected Areas in Communications, IEEE Journal on*, vol. 30, no. 3, pp. 575–585, 2012.

[8] G. Nigam, P. Minero, and M. Haenggi, "Coordinated Multipoint Joint Transmission in Heterogeneous Networks," *IEEE Transactions on Communications*, 2014, submitted. Available at http://www.nd.edu/~mhaenggi/pubs/tcom14.pdf.

[9] W. Lei, W. Hai, Y. Yinghui, and Z. Fei, "Heterogeneous network in LTE-advanced system," in *Communication Systems (ICCS), 2010 IEEE International Conference on*. IEEE, 2010, pp. 156–160.

[10] C.-H. Lee and M. Haenggi, "Interference and outage in Poisson cognitive networks," *Wireless Communications, IEEE Transactions on*, vol. 11, no. 4, pp. 1392–1401, 2012.

[11] 3GPP:R1-100701, "Importance of serving cell association in HetNets," *Qualcomm Inc.*, Jan. 2010.

[12] M. Haenggi, "Mean interference in hard-core wireless networks," *Communications Letters, IEEE*, vol. 15, no. 8, pp. 792–794, 2011.

[13] R. Ganti and M. Haenggi, "Interference and outage in clustered wireless ad hoc networks," *Information Theory, IEEE Transactions on*, vol. 55, no. 9, pp. 4067–4086, 2009.